Title: Juvenile antioxidant treatment prevents adult deficits in a developmental model of schizophrenia.
Authors: Cabungcal JH, Counotte DS, Lewis EM, Tejeda HA, Piantadosi P, Pollock C, Calhoon GG, Sullivan EM, Presgraves E, Kil J, Hong LE, Cuenod M, Do KQ, O'Donnell P
Journal: Neuron
Year: 2014 Sep 3
Volume: 83
Issue: 5
Pages: 1073-84
DOI: 10.1016/j.neuron.2014.07.028

HHS Public Access

Author manuscript

Neuron. Author manuscript; available in PMC 2015 September 03.

Published in final edited form as:

Neuron. 2014 September 3; 83(5): 1073–1084. doi:10.1016/j.neuron.2014.07.028.

Juvenile antioxidant treatment prevents adult deficits in a developmental model of schizophrenia

Jan Harry Cabungcal[#1], **Danielle S. Counotte**[#3], **Eastman Lewis**[#2,3], **Hugo A. Tejeda**[2,3], **Patrick Piantadosi**[3], **Cameron Pollock**[3], **Gwendolyn G. Calhoon**[2,3], **Elyse Sullivan**[2,3], **Echo Presgraves**[3], **Jonathan Kil**[4], **L. Elliot Hong**[2,5,6], **Michel Cuenod**[1], **Kim Q Do**[1,¶], and **Patricio O'Donnell**[2,3,5,¶]

[1] Centre for Psychiatric Neuroscience, Department of Psychiatry, Lausanne University Hospital, Lausanne, Switzerland [2] Program in Neuroscience, University of Maryland School of Medicine, Baltimore, MD, USA [3] Department of Anatomy & Neurobiology, University of Maryland School of Medicine, Baltimore, MD, USA [4] Sound Pharmaceuticals, Inc, Research and Development, Seattle, WA, USA [5] Department of Psychiatry, University of Maryland School of Medicine, Baltimore, MD, USA [6] Maryland Psychiatric Research Center, Baltimore, MD, USA

[#] These authors contributed equally to this work.

SUMMARY

Abnormal development can lead to deficits in adult brain function, a trajectory likely underlying adolescent-onset psychiatric conditions such as schizophrenia. Developmental manipulations yielding adult deficits in rodents provide an opportunity to explore mechanisms involved in a delayed emergence of anomalies driven by developmental alterations. Here we assessed whether oxidative stress during presymptomatic stages causes adult anomalies in rats with a neonatal ventral hippocampal lesion, a developmental rodent model useful for schizophrenia research. Juvenile and adolescent treatment with the antioxidant N-acetyl cysteine prevented the reduction of prefrontal parvalbumin interneuron activity observed in this model, as well as electrophysiological and behavioral deficits relevant to schizophrenia. Adolescent treatment with the glutathione peroxidase mimic ebselen also reversed behavioral deficits in this animal model. These findings suggest that presymptomatic oxidative stress yields abnormal adult brain function in a developmentally compromised brain, and highlight redox modulation as a potential target for early intervention.

[¶]Correspondence to: patricio.odonnell@pfizer.com; kim.do@chuv.ch..

Author contributions: MC, KQD, and POD designed the experiments; JHC, DSC, EL, HAT, PP, CP, GGC, ES, EP conducted experiments; JHC, DSC, EL, HAT, ES, KQD, POD, analyzed the data; JK and LEH provided materials; JHC, DSC, MC, KQD, POD wrote the manuscript.

All other authors have nothing to disclose.

INTRODUCTION

Developmental insults can yield adolescent or adult brains with heightened vulnerability to deleterious environmental factors, an interaction likely to play a role in neuropsychiatric disorders of adolescent onset (O'Donnell, 2011). Despite intense research efforts, we still do not understand the mechanisms that could link genetic risk and early developmental disturbances with adult deficits. Among the hypotheses being advanced, oxidative stress stands out as a strong possible mechanism (Cabungcal et al., 2013b; Do et al., 2009; O'Donnell, 2012b). This idea is supported by the observation of various polymorphisms in genes encoding glutathione (GSH) synthesis conferring risk for schizophrenia (Gysin et al., 2007; Tosic et al., 2006). GSH, the most abundant endogenous antioxidant, is responsible for maintaining cellular oxidative balance (Do et al., 2009). Decreased GSH levels have been observed in peripheral tissues, cerebrospinal fluid, and postmortem brains of schizophrenia patients (Do et al., 2000; Gawryluk et al., 2011; Yao and Keshavan, 2011), and the GSH precursor *N*-acetyl cysteine (NAC) increases peripheral GSH levels and improves neurophysiological deficits in patients (Berk et al., 2008; Carmeli et al., 2012; Lavoie et al., 2008). Furthermore, brain GSH levels assessed with magnetic resonance spectroscopy are decreased in the prefrontal cortex (PFC) of patients with schizophrenia (Do et al., 2000). However, while mounting evidence does suggest a role of oxidative stress in schizophrenia, the time course and neural substrates of oxidative stress induced by developmental disturbances are not well understood, and whether oxidative stress is causal to behavioral deficits remains to be determined.

Several rodent models have been designed to test possible developmental pathophysiological scenarios in major psychiatric disorders. Mice with GSH deficit or mitochondrial dysfunction, for example, show schizophrenia-related electrophysiological, morphological, and behavioral anomalies (Steullet et al., 2010). As these deficits are reversed with NAC (Cabungcal et al., 2013a; Otte et al., 2011), GSH is likely critical for proper postnatal brain maturation. Another example is the latent neuropathological alteration induced by maternal immune activation, which becomes evident when combined with juvenile social isolation (Giovanoli et al., 2013). A widely used tool to assess developmental trajectories of adult-onset prefrontal cortical deficit is the neonatal ventral hippocampal lesion (NVHL). This procedure yields adult animals with PFC-dependent electrophysiological, neurochemical, and behavioral anomalies related to phenomena observed in schizophrenia, all of which emerge during adolescence (O'Donnell, 2011; Tseng et al., 2009). Of note, NVHL rats show altered prefrontal inhibitory interneuron maturation during adolescence (Tseng et al., 2008), highlighting this as a model of developmentally induced, late-onset alterations in prefrontal cortical excitation-inhibition balance. The NVHL is therefore a useful tool to test whether oxidative stress is responsible for adult deficits in a model that does not directly manipulate GSH or alter redox status, which is important to determine whether oxidative stress is a consequence of developmental cortical deficits. Here, we tested whether antioxidant treatment with NAC during juvenile and adolescent periods affects maturation of NVHL rats; the aim was to assess whether restoring redox balance prevented adult deficits in a developmentally compromised brain.

RESULTS

One of the most replicated findings in schizophrenia research is a reduction of markers associated with cortical inhibitory interneurons (Lewis et al., 2012). Adult NVHL rats exhibit electrophysiological anomalies caused by altered cortical interneuron maturation, characterized by abnormal modulation by dopamine (Tseng et al., 2008). We tested whether parvalbumin (PV) positive interneurons in the PFC, including the dorsal prelimbic and anterior cingulate cortex (ACC), are altered in NVHL rats using unbiased stereological counting techniques. Between postnatal day (P) 21 and P61, the number of PV immunoreactive interneurons (PVI) increased in sham-operated rats, but not in NVHL rats (Figure 1A, B). In juvenile rats (P21), there was no significant difference in PVI counts between NVHL and sham rats, but adult (P61) NVHL rats showed significantly fewer PVI in the PFC compared to sham rats. The PVI reduction was prevented with NAC treatment starting at P5 (i.e., 2 days prior to the hippocampal lesion) and lasting into adolescence (P50; Figure 1A-C), suggesting juvenile oxidative stress induced by the neonatal lesion impairs PVI maturation. Caspase 3 labeling did not reveal apoptotic activation in the PFC of NVHL rats (data not shown), suggesting that reduced PVI immunoreactivity more likely reflects reduced interneuron activity than cell loss.

To assess oxidative stress, we quantified DNA oxidation with 8-oxo-7, 8-dihydro-20-deoxyguanine (8-oxo-dG) labeling. At P21, NVHL rats exhibited a massive increase in 8-oxo-dG staining in the PFC compared to sham rats, in both pyramidal neurons and interneurons, which was completely prevented by NAC treatment (Figure 2A, B). When NVHL rats reached adulthood (P61), they still showed increased 8-oxo-dG, albeit less than at P21 (Figure 2C, D). We also observed an increase in 3-Nitrotyrosine (3-NT) levels in adult PFC of NVHL rats. 3-NT indicates nitration of proteins due to oxidative and nitrosative stress (Radi, 2004), and its increase in NVHL rats was prevented by NAC treatment during development (Figure 3). Thus, juvenile NAC treatment decreased multiple markers of oxidative stress in adult NVHL rats to levels comparable to control rats, without affecting the extent of the lesion (Figure S1). A possible explanation for the levels of oxidative stress detected in the adult PFC following an NVHL is the reduced glutamatergic input from ventral hippocampus during development, as blocking NMDA receptors induces oxidative stress in PVI (Behrens et al., 2007). Our data indicate that impairing hippocampal inputs to the PFC during a critical developmental period elicits PFC oxidative stress in juvenile rats that has deleterious effects on the adolescent maturation of PVI.

To determine the types of interneurons expressing oxidative stress in NVHL rats, we co-labeled 8-oxo-dG with PV, calbindin (CB) and calretinin (CR). In addition to pyramidal neurons, increased 8-oxo-dG staining was observed in PVI, but not in CB or CR interneurons (Figure 4). About 50% of PVI were co-labeled with 8-oxo-dG, indicating oxidative stress is pervasive in this cell population. A marker of PVI maturation is *Wisteria Floribunda agglutinin* (WFA), a lectin that recognizes the perineuronal nets (PNN) enwrapping mature cortical PVI. The NVHL lesion reduced WFA staining (Figure 5), suggesting that PVI in adult PFC of NVHL rats show an immature phenotype. These extracellular matrix alterations were restored with juvenile NAC treatment (Figure 5). PVI may be highly exposed to increased oxidative stress because they make up the majority of

fast-spiking interneurons and their high energy metabolism may generate more reactive oxygen species than non-fast spiking neurons. It is possible that juvenile PVI are functional while exhibiting oxidative stress, with the deleterious effects of oxidative stress becoming evident upon periadolescent PVI maturation.

If juvenile oxidative stress is the cause of physiological anomalies observed in adult NVHL rats, NAC treatment should rescue these alterations. We conducted whole-cell recordings from pyramidal neurons in adult brain slices containing the medial PFC of SHAM (n=12), NVHL (n=16), and NAC-treated NVHL rats (n=14). As previously shown in adult NVHL rats and other rodent models of schizophrenia (Niwa et al., 2010; Tseng et al., 2008), the dopamine D2-dependent modulation of excitatory postsynaptic potentials (EPSPs) in layer V pyramidal cells was lost in NVHL rats (Figure 6A-C). This loss is likely due to abnormal maturation of PFC interneurons, as the normal adult D2 modulation includes a GABA-A receptor component (Tseng and O'Donnell, 2007), but oxidative stress in pyramidal neurons may also play a role. To determine whether altered PVI-dependent PFC synaptic responses are due to oxidative stress, rats were treated with NAC during development and then tested for D2 modulation of PFC physiology. NAC treatment rescued the D2 modulation of synaptic responses in NVHL rats (Figure 6A-C), indicating that juvenile and adolescent oxidative stress in NVHL rats alters function of local circuits in the adult PFC.

The abnormal dopamine modulation of PFC function in NVHL rats is also observed *in vivo*. We performed *in vivo* intracellular recordings in 38 pyramidal neurons from adult rats (n=9 SHAM, n=5 NVHL, and n=7 NAC-treated NVHL). Baseline activity was consistent with what has been previously reported for PFC pyramidal neurons (Lewis and O'Donnell, 2000), and was not significantly affected by lesion status or NAC treatment. All recorded cells exhibited spontaneous transitions between the resting membrane potential (down state; −76.2 ± 1.1 mV) and the up state (−67.6 ± 0.7 mV). Up states occurred at a frequency of 0.6 ± 0.1 Hz with a duration of 523.6 ± 24.7 ms. The majority of cells (n=21) fired spontaneously at a rate of 2.1 ± 0.7 Hz. As previously reported (O'Donnell et al., 2002), *in vivo* intracellular recordings from anesthetized adult NVHL rats revealed an abnormal increase in pyramidal cell firing in response to burst stimulation of the Ventral Tegmental Area (VTA) (Figure 6D, E) compared to sham rats. This abnormal increase in firing was prevented by juvenile NAC treatment (Figure 6D, E). These data indicate that abnormal dopamine function in the PFC of NVHL rats depends on oxidative stress during juvenile and adolescent stages.

Abnormal cortical synaptic function in adult NVHL rats should yield altered information processing that would be prevented by NAC treatment if it depended on oxidative stress. We tested mismatch negativity (MMN) using auditory evoked potentials in an oddball paradigm in SHAM (n=6), NVHL (n=3), and NAC-treated NVHL rats (n=3). MMN has high translational relevance, as it is attenuated in schizophrenia patients (Javitt et al., 1993) and in animal models (Ehrlichman et al., 2009). We implanted EEG electrodes in NVHL, NAC-treated NVHL, and sham rats. MMN was significantly different among groups, with NAC treatment improving MMN in NVHL rats (Figures 7A, B). This observation is consistent with the effect of NAC on MMN in patients (Lavoie et al., 2008), and indicates the NVHL model reproduces an important disease marker that can be prevented by juvenile antioxidant

treatment. As MMN depends on NMDA receptor function (Umbricht et al., 2000) and NMDA hypofunction in PVI is suspected in schizophrenia, it is possible that MMN improvement with NAC results from restored PVI activity.

To assess whether juvenile oxidative stress leads to behavioral deficits, we used a behavioral paradigm tested in both animal models and schizophrenia patients. Prepulse inhibition of the acoustic startle response (PPI) is a measure of sensorimotor gating that is reduced in patients (Geyer and Braff, 1987) and NVHL rats (Lipska et al., 1995). We tested PPI in adult sham (n=11), NAC-treated sham (n=12), NVHL (n=9), and NAC-treated NVHL rats (n=17). Juvenile NAC treatment prevented the reduced PPI observed in untreated NVHL rats (Figure 8A). In addition to loss of PVI maturation and electrophysiological anomalies, developmental oxidative stress in juvenile NVHL rats can cause schizophrenia-relevant adult behavioral deficits.

The beneficial effect of NAC treatment reported above includes a large postnatal treatment that starts prior to the lesion and stops once rats become young adults. For these results to have a full translational value, it is critical to determine whether NAC is efficacious when started at an age that corresponds to the time when prodromal stages can be identified in humans. In another set of rats, we administered NAC in the drinking water starting at P35, an age that in rats is equivalent to early adolescence. We tested for PPI deficits in adult sham (n=15), untreated NVHL (n=12), and NAC-treated NVHL rats (n=14). Although there was only a trend for a deficit in untreated NVHL rats compared to shams in this group, there was a significant difference between untreated and treated NVHL (Figure 8B). The data indicate that GSH precursors such as NAC can still be effective even if initiated after oxidative stress has begun.

One important caveat of NAC is that it also alters glutamate levels by virtue of its action on the cysteine-glutamate transporter (Moussawi et al., 2009). To test whether redox modulation and not glutamate level changes were responsible for NAC effects in NVHL rats, we assessed the effect of two other antioxidants that do not alter glutamate. Ebselen is a glutathione peroxidase (GPx) mimic (Muller et al., 1984) that induces GPx expression (Kil et al., 2007) and enhances GSH levels in neurons, replenishing GSH depleted by neurotoxic mechanisms (Pawlas and Malecki, 2007). We tested PPI in adult vehicle-treated SHAM (n=10), ebselen-treated SHAM (n=7), vehicle-treated NVHL (n=8), and ebselen-treated NVHL rats (n=9). Ebselen treatment during adolescence reversed PPI deficits in NVHL rats (Figure 8C). In another group of rats, we assessed the effects of the NADPH oxidase inhibitor and antioxidant apocynin, in this case delivered through juvenile and adolescent stages. We tested PPI in adult vehicle-treated SHAM (n=10), apocynin-treated SHAM (n=11), vehicle treated NHVL (n=7), and apocynin-treated NVHL (n=5). We again observed a reversal of PPI deficits (Figure 8D). The data indicate that elevation of GSH and not glutamate during adolescence rescues PPI deficits in NVHL rats.

DISCUSSION

We observed increased level of oxidative stress immunolabeling in the PFC of juvenile NVHL rats, along with a decrease in PV cell counts, PPI deficit, altered dopamine

modulation of local PFC circuits, and deficits in evoked-related potentials in the EEG of adult NVHL rats. All these deficits were prevented with NAC treatment from P5 to P50. PPI deficits were also prevented if NAC treatment was initiated during adolescence (P35) and by two other redox modulators. Our data suggest that oxidative stress in prefrontal cortex is a core feature mediating alterations induced by the NVHL, and antioxidant treatment prevents these alterations. Presymptomatic oxidative stress, highly present in PVI and also observed in pyramidal neurons, is therefore responsible for diverse schizophrenia-relevant phenomena in a neurodevelopmental model that does not entail a direct manipulation of redox pathways.

Oxidative stress can affect PFC function via several mechanisms. With high levels of oxidative stress, cell damage or death can occur via membrane lipid peroxidation, DNA mutagenesis, alterations in chromatin structure, inactivation of critical enzymes, or activation of kinase and caspase cascades (Bitanihirwe and Woo, 2011). Redox imbalance can also lead to brain development disturbances by affecting redox-sensitive cysteine residues at the DNA-binding sites of transcription factors (Haddad, 2002) and affecting mitochondrial DNA, highly susceptible to oxidation (Jones and Go, 2010). Furthermore, many synaptic proteins include regulatory redox sites; for example, NMDA receptors become hypofunctional following oxidation (Steullet et al., 2006). We detected oxidative stress and nitrosative stress in PFC pyramidal neurons and PVI in juvenile rats with a NVHL prior to the onset of electrophysiological and behavioral deficits. This indicates PVI may still be somewhat functional, and that upon their periadolescent maturation the deleterious effect of oxidative stress renders them into a diseased state as revealed by the reduction in PV and PNN labeling. Our data indicate that redox alterations in the NVHL model encompass both oxidative and nitrosative stress, and treatments that increase GSH (NAC and ebselen) or decrease reactive oxygen species (ROS) generation (ebselen and apocynin) prevent adult-onset behavioral deficits. The increases in 3NT levels point to dysregulation of nitric oxide (NO) and arginine signaling, as well as nitrosative stress, as reported in schizophrenia (Yao et al., 2004). Whether this dysregulation implicates the various isoforms of NO synthase (nNOS, eNOS, or iNOS) is still unknown. Thus, the NVHL model presents a widespread alteration in redox pathways that could be reversed by targeting different modulators, such as GSH, GPx, and NADPH oxidase.

Oxidative stress is also seen in another animal model of schizophrenia: the dominant negative DISC1 (DN-DISC1) mouse (Johnson et al., 2013). Similar to our findings, DN-DISC1 mice show increased 8-oxo-dG staining in the PFC that is associated with several behavioral deficits (Johnson et al., 2013). Our results add to this observation by showing a causal link between heightened oxidative stress in the PFC and the electrophysiological and behavioral deficits associated with schizophrenia, as the anti-oxidant NAC prevents both the increase in oxidative stress and electrophysiological and behavioral deficits in NVHL rats.

PFC physiology was dysfunctional in adult NVHL rats, and this deficit was prevented by NAC treatment. We used several endpoints to assess PFC function, including dopamine modulation of synaptic responses in pyramidal neurons in slices, *in vivo* intracellular recordings of responses to VTA stimulation, and auditory evoked potentials. Recordings from pyramidal neurons showed loss of D2-mediated attenuation of cortico-cortical EPSPs in slices and exaggerated firing evoked by VTA stimulation *in vivo* in adult NVHL rats, as

we had reported previously (O'Donnell et al., 2002; Tseng et al., 2008). Both the slice D2 attenuation of pyramidal cell synaptic responses and the *in vivo* silencing of pyramidal neurons by VTA stimulation are dependent on activation of FSI by dopamine in naïve rats (Tseng and O'Donnell, 2007). The absence of alterations in these responses in NAC-treated NVHL rats indicates that oxidative stress during postnatal development has a deleterious effect on dopamine-modulated FSI-pyramidal cell interactions. Currently, there is a debate as to whether interneurons or pyramidal neurons are the primary site of dysfunction in schizophrenia. Our data are agnostic to which cell type is primarily affected and highlights oxidative stress as a cause of altered interactions between pyramidal neurons and inhibitory interneurons.

Oxidative stress could be brought up in the NVHL model by a number of mechanisms. First, this could be the result of the administration of an excitotoxic agent, such as ibotenic acid. Our previous work showing that neonatal ventral hippocampal injection of the bacterial endotoxin LPS yielded anomalies similar to the NVHL (Feleder et al., 2010) suggests this could be the case. However, a variation of this model in which the hippocampus was just reversibly inactivated produces similar behavioral alterations as the lesion (Lipska et al., 2002), suggesting the excitotoxic damage in the NVHL may not be what causes the deficits. It is more likely that the loss of hippocampal-prefrontal synaptic activity and/or the loss of trophic factors in the PFC induced by the loss of hippocampal inputs during a critical developmental stage may affect the developing prefrontal cortical neurons. This possibility is supported by work by Margarita Behrens showing that NMDA receptor antagonists can induce oxidative stress in PV interneurons (Behrens et al., 2007; Behrens et al., 2008). Thus, oxidative stress in NVHL rats may be a consequence of network developmental alterations.

Mismatch negativity is a measure of high translational relevance. MMN tests the attribution of saliency to deviant auditory stimuli, and it is disrupted in schizophrenia patients (Javitt et al., 1993). Here, we report MMN deficits in NVHL rats, which are prevented by NAC treatment. As MMN is dependent on NMDA receptor activity (Ehrlichman et al., 2009), it is likely that oxidative stress impairs NMDA-dependent synaptic cortical mechanisms involved in processing of salient vs. common signals. The functional assessment of the impact of antioxidant treatment was complemented by testing of sensorimotor integration with PPI. Both juvenile and adolescent-only NAC treatment prevented adult PPI deficits in NVHL rats. The observation that adolescent treatment with NAC or ebselen is sufficient to prevent PPI deficits has important implications for redox mechanisms as potential targets for schizophrenia treatment. We showed that it is possible to prevent or reverse a deficit even if antioxidant treatment is initiated after the development of oxidative stress. As ultra-high risk subjects for schizophrenia cannot be identified until adolescence, our finding keeps open the possibility that redox modulation can be beneficial even if initiated once high risk has been identified.

Our data reveal that presymptomatic oxidative stress can cause aberrant adult PFC function in NVHL rats. This developmental manipulation is a well-established model of altered cortical excitation-inhibition balance. As is the case with any schizophrenia- related models, the NVHL should not be seen as reproducing the disease (there is no such thing as a schizophrenic rat). In addition, the model entails a lesion, which is not observed in

schizophrenia. However, the NVHL and other developmental models have been useful to test specific hypotheses about developmental trajectories of electrophysiological and behavioral phenomena of relevance to the disease (O'Donnell, 2013). Major strengths of the NVHL model include the adolescent onset of deficits and the ability to reproduce phenomena observed in schizophrenia when translatable measures are evaluated (O'Donnell, 2012a). Remarkably, the NVHL model converges with several other manipulations used as animal models for schizophrenia research in producing loss of PVI immunolabeling and altered excitation-inhibition balance (O'Donnell, 2011). Despite their limitations, the behavioral and physiological endpoints we used here are widely used to assess integrity of cortical inhibitory networks and their impact on pyramidal cell activity. Inhibitory networks, developing at the time of the lesion and beyond, play a crucial role in experience-dependent refinement of neural networks (Hensch, 2005) that extends into adolescence. This role may be reflected in cognitive training during adolescence preventing cognitive impairments in adult NVHL rats (Lee et al., 2012) and adolescent stress unmasking latent neuropathology in mice with maternal immune activation (Giovanoli et al., 2013). Adolescence is therefore a critical developmental stage in which pathophysiological conditions involving oxidative stress can affect a still developing PFC, but it yet provides a window of opportunity for therapeutic intervention. This suggests that antioxidants or redox regulators without serious side effects may prove effective to reduce conversion in subjects at risk for psychiatric disorders by preventing pathophysiological changes associated with loss of cortical pyramidal cell and PVI function.

Experimental Procedures

Animals

Timed-pregnant Sprague-Dawley rats were obtained at gestational days 13-15 from Charles River (Wilmington, MA) and were individually housed with free access to food and water in a temperature- and humidity-controlled environment with a 12:12h light/dark cycle (lights on at 7:00 AM). When pups reached P5, half of the dams received NAC in their drinking water. Pups were left undisturbed until P7-9 when healthy offspring were randomly separated and received either NVHL or sham surgery. At P21, male and female pups were either transcardially perfused with 4% paraformaldehyde for immunocytochemistry or weaned and housed in groups of two to three, counterbalanced across lesion status. NAC treatment lasted throughout adolescence until P50. After reaching adulthood (>P60), animals were either perfused with 4% paraformaldehyde for immunocytochemistry, perfused with artificial cerebrospinal fluid (aCSF) for slice electrophysiology, utilized for *in vivo* intracellular recordings, or tested for PPI or MMN. All experiments were approved by the University of Maryland School of Medicine Institutional Animal Care and Use Committee.

Neonatal ventral hippocampal lesion surgery

Between P7 and P9, pups (15-20 g) received either an excitotoxic lesion of the ventral hippocampus (NVHL) or sham procedure, as previously described (Chambers and Lipska, 2011). Pups were anesthetized with hypothermia and secured to a Styrofoam platform attached to a stereotaxic frame (David Kopf Instruments, Tujunga, CA). NVHL rats received a bilateral infusion of ibotenic acid (10 μg/μl in aCSF, 0.3 μl/side; Tocris, Minneapolis, MN)

into the ventral hippocampus (3 mm rostral to Bregma, 3.5 mm lateral to midline, and 5 mm from surface) at a rate of 0.15 μl/min. Sham surgeries were done in exactly the same fashion, but the guide cannula was lowered only 3 mm and without any liquid infusion to control for the surgical procedure while avoiding hippocampal damage. After the surgery, wounds were clipped and when pups activity level had returned to normal, they were returned to their dams and remained undisturbed until the wound clips were removed and rats weaned at P21.

In all rats, lesions were verified by sectioning (40 μm) the dorsal and ventral hippocampus using a freezing microtome. Sections were mounted on glass slides and Nissl stained. The hippocampus was examined microscopically for evidence of bilateral damage, which typically included cell loss, thinning, gliosis, cellular disorganization and enlarged ventricles (Chambers and Lipska, 2011).

Antioxidant pretreatment regimen

NAC (BioAdvantexPharma, Mississauga, Ontario, Canada) was administered in the drinking water at 900 mg/l. NAC treatment started at P5 or at P35, and previous work in mice has shown that NAC consumed by the dam is transmitted to the pups through her milk (das Neves Duarte et al., 2012). NAC treatment ended at P50. Fresh solutions were prepared every 2-3 days. Ebselen (Sound Pharmaceuticals Inc., Seattle, WA) was administered i.p. 5 days a week starting at P35 until the day of PPI testing (P60). Stock ebselen solution (20 mg/ml DMSO, frozen aliquots) was diluted 1:5 in sterile water and administered at a dose of 10 mg/kg. Control animals received an equivalent concentration of DMSO diluted 1:5 in water. Apocynin (Sigma-Aldrich, St. Louis, MO) was administered in the drinking water at a target dose of 100 mg/kg (Nwokocha et al., 2013). Prior to weaning at P21, drinking water contained a dose of 2 g apocynin per 0.5 l of water, to ensure delivery through the dam's milk. Apocynin concentration was lowered after weaning to 750 mg/l to best approximate the target dose. Treatment lasted from P5 to P50 with fresh solutions prepared every other day.

Immunohistochemistry

Immunohistochemistry and stereological quantification—A total of 18 (P21) and 25 (P61) male rats were anesthetized, perfused and their brains fixed as previously described (Cabungcal et al., 2006). Coronal sections (40 μm) were used to investigate the inhibitory circuitry of anterior cingulate cortex (ACC). Brain sections were immunolabeled for parvalbumin (PV) as described previously (Steullet et al., 2010). PV-immunoreactive cell (cell bodies) count was quantified in ACC using the StereoInvestigator 7.5 software (MBF Bioscience Inc, Williston, VT, USA). Briefly, stereological counting started with low magnification (x2.5 objective) to identify and delineate the boundaries of the region of interest (ROI) on 2-4 consecutive sections from each animal. The ACC (at Bregma approximately 0.70-1.70 mm) was delineated from the secondary motor (M2) cortical regions following the anatomical cytoarchitectonic areas given by Paxinos and Watson (Paxinos and Watson, 1998). The selected region of interest (ROI) included the majority of the cingulate cortex area 1 (cg1) and part of cingulate cortex area 2 (cg2). A small intermediate allowance was set between ACC and M2 regions to ensure that the ROI in ACC did not overlap with the secondary motor cortex. A counting box (optical dissector)

within the section thickness and sampling frames adapted to ACC were used to analyze and count neurons (Schmitz and Hof, 2005). The counting boxes (40 x 40 μm with 15 μm in depth) were placed by the software in each sampling frame starting from a random position inside the ROI of the ACC. Counting was carried out using higher magnification (x40 objective). PV cells were counted when they were in focus at the surface of the box until out of focus at 15-μm depth of the counting box. A 5-μm guard zone was used to distance from artifacts that can be influenced by tissue shrinkage due to the immunopreparation processing. We used 25 counting frames in the ROI volume of the ACC for P21 and P61 rats.

Immunofluorescence staining, confocal microscopy and image analysis— Oxidative stress was visualized using an antibody against 8-oxo-7, 8-dihydro-20-deoxyguanine (8-Oxo-dG), a DNA adduct formed by the reaction of OH radicals with the DNA guanine base (Kasai, 1997). Because of the proximity of the electron transport chain, mitochondrial DNA is prone to oxidative damage: levels of oxidized bases in DNA and levels of 8-oxo-dG are higher in mitochondria than in the nucleus. To assess 8-oxodG and 3-Nitrotyrosine (3NT) labeling in various types of interneurons, coronal sections between Bregma 0.70-1.70 mm were incubated for about 36 hours with rabbit polyclonal anti-PV, anti-calbindin-28k (anti-CB), or anti-calretinin (anti-CR) (1:2500; Swant, Bellinzona, Switzerland) primary antibodies together with the mouse monoclonal anti-8-oxo-dG (1:350; AMS Biotechnology, Bioggio-Lugano, Switzerland) primary antibody or mouse monoclonal anti-nitrotyrosine (1:1000; Chemicon International, Temecula, USA) primary antibody. To enable visualization of the PNN that surrounds PV cells, sections were incubated in a solution containing the biotin-conjugated lectin *Wisteria floribunda agglutinin* (WFA) (Hartig et al., 1994). Sections were first incubated with PBS + Triton 0.3% + sodium azide (1 g/l) containing 2% normal horse serum, followed by 36-hour incubation with rabbit polyclonal anti-PV (1:2500) and biotin conjugated-WFA (1:2000; Sigma). Sections were washed, incubated with appropriate fluorescent secondary antibodies (goat anti-mouse immunoglobulin G (1:300; Alexa Fluor 488; Molecular Probes, Eugene, Oregon), anti-rabbit immunoglobulin G (1:300; CY3; Chemicon International, Temecula, California), CY2-Streptavidin conjugate (1:300; Chemicon), and counterstained with 100 ng/ml DAPI (4'-6-diamidino-2-phenylindole; Vector Laboratories, California, USA). Sections were visualized with a Zeiss Confocal Microscope equipped with x10, x20, x40 and x63 Plan-NEOFLUAR objectives. All peripherals were controlled with LSM 510 software (Carl Zeiss AG, Switzerland). Z stacks of 9 images (with a 2.13 μm interval) were scanned (1024 × 1024 pixels) for analysis in IMARIS 7.3 software (Bitplane AG, Switzerland). All images of Z stacks were filtered with a Gaussian filter tool to remove unwanted background noise and sharpen cell body contours. An ROI as defined in the stereological procedure was created in ACC. The ROI was masked throughout the Z stacks to isolate regional subvolumes of the ACC in which PV-, CB-, and CR-expressing interneurons were analyzed. To quantify 8-oxo-dG, the staining intensity and number of labelled voxels within the ROI were measured. To quantify 8-oxo-dG in PV-, CB- and CR-cells, we used the *Coloc* module of the IMARIS software to calculate the proportion of all PV-immunolabeled voxels (respectively, CB- and CR-immunolabeled voxels), which were also 8-oxo-dG-immnolabeled. *Coloc* gives the count of colocalized voxels between the immunolabeled profiles of interest. To quantify the

number of PV immunoreactive neurons surrounded by PNN, we used the spots module to assign spot markings on profile-labelled voxels that fall within a given size. The channels for PV and WFA immunolabeling were chosen, and profile size criterion (>9 and 4 μm, respectively) was defined to quantify labelled profiles above these sizes. Spots generated for PV that contacted and/or overlapped with spots generated for WFA were considered as those PVI surrounded by PNN (WFA-positive PVI).

Slice electrophysiology

Starting at P60, male rats were anesthetized with chloral hydrate (400 mg/kg, i.p.) 15 min before being decapitated. Brains were quickly removed from the skull into ice-cold artificial CSF (aSCF) oxygenated with 95% O_2-5% CO_2 and containing the following (in mM): 125 NaCl, 25 $NaHCO_3$, 10 glucose, 3.5 KCl, 1.25 NaH_2PO_4, 0.1 $CaCl_2$ and 3 $MgCl_2$, pH 7.45 (295-300 mOsm). Coronal slices (300 μm thick) containing the medial PFC were obtained with a vibratome in ice-cold aCSF and incubated in warm (~35°C) aCSF solution constantly oxygenated with 95% O_2-5% CO_2 for at least 45 min before recording. The recording aCSF (with 2 $CaCl_2$ and 1 $MgCl_2$) was delivered to the recording chamber with a pump at the rate of 2 ml/min.

Patch electrodes (7-10 MΩ) were obtained from 1.5 mm borosilicate glass capillaries (World Precision Instruments) with a Flaming-Brown horizontal puller (P97; Sutter Instruments) and filled with a solution containing 0.125% Neurobiotin and the following (in mM): 115 K-gluconate, 10 HEPES, 2 $MgCl_2$, 20 KCl, 2 MgATP, 2 Na_2-ATP, and 0.3 GTP, pH 7.25-7.30 (280-285 mOsm). Quinpirole (5 μM, Tocris) was freshly mixed into oxygenated recording aCSF every day before an experiment. Both control and drug-containing aCSF were oxygenated continuously throughout the experiments.

All experiments were conducted at 33-35°C and prelimbic or ACC PFC pyramidal cells from layer V were identified under visual guidance using infrared (IR) differential interference contrast video microscopy with a 40X water-immersion objective (Olympus BX-51WI). The image was detected with an IR-sensitive CCD camera and displayed on a monitor. Whole-cell current-clamp recordings were performed with a computer-controlled amplifier (Multiclamp 700A; Molecular Devices), digitized (Digidata 1322; Molecular Devices), and acquired with Axoscope 9 (Molecular Devices) at a sampling rate of 10 kHz. Electrode potentials were adjusted to zero before recording without correcting the liquid junction potential. Baseline activity in each neuron was monitored for 10 minutes during which membrane potential and input resistance (measured with the slope of a current-voltage (I/V) plot obtained with 500-ms-duration depolarizing and hyperpolarizing pulses) were measured.

Synaptic responses were tested in pyramidal neurons with electrical stimulation of superficial layers with a bipolar electrode made from a pair of twisted Teflon-coated Tungsten wires (tips separated by ~200 μm) and placed ~500 μm lateral to the vertical axis of the apical dendrite of the recorded neuron. Stimulation pulses (20-400 μA; 0.5 ms) were delivered every 15 s. The intensity was adjusted to evoke EPSPs with about half of the maximal amplitude. Throughout the experiment, changes in input resistance were monitored with repeated hyperpolarizing steps, and the cell was discarded when input resistance

changed more than 20% during the course of the experiment. The amplitude of evoked EPSPs was measured with Clampfit 9.0 and averaged over 10 sweeps before and after 7 minutes of application of quinpirole. This period was chosen for consistency, with differences revealed by previous investigations of D2 modulation of PFC activity in rodent models of schizophrenia (Niwa et al., 2010; Tseng et al., 2008). At the end of each experiment, slices were placed in 4% paraformaldehyde and processed for DAB staining using standard histochemical techniques to verify morphology and location of the neurons.

In Vivo intracellular recordings

Female rats were anesthetized with choral hydrate (400 mg/kg, i.p) and placed on a stereotaxic apparatus (Kopf Instruments). Anesthesia was maintained through recording procedures with continuous choral hydrate (24-30 mg/kg/h) via an intraperitoneal catheter. Body temperature was maintained at approximately 37°C using a thermal probe-controlled heat pad (Fine Science Tools). Concentric bipolar stimulating electrodes (0.5 mm diameter, 0.5 mm pole separation; Rhodes Medical Instruments Inc.) were lowered into the VTA (5.8 mm caudal to bregma; 0.5-0.8 mm lateral to midline; 7-8 mm from surface) for stimulation. Recording sharp micro-electrodes were pulled from borosilicate glass (1 mm O.D.; World Precision Instruments) on a horizontal Flaming-Brown puller (Sutter Instruments). Sharp electrodes (50-110 MΩ) were filled with 2% Neurobiotin (Vector Laboratories) in 2M potassium acetate. Microelectrodes were lowered into the medial PFC using a hydraulic manipulator (Trent Wells, Coulterville, CA). Recordings were made in current clamp, and signals were acquired using a Neurodata Amplifier (Cygnus), digitized at 10 kHz using a Digidata A/D converter (Molecular Devices) and Axoscope 9 software (Molecular Devices) for offline analyses.

Microelectrodes were advanced through the medial PFC until a neuron was impaled. Neurons included in this study had a resting membrane potential more negative than – 60 mV and action potentials with amplitudes ≥ 40 mV from threshold. To determine responses to endogenous dopamine, the VTA was stimulated with trains of 5 pulses at 20 Hz, delivered every 10 seconds. Eight to ten sweeps were used to determine cell firing in response to VTA stimulation. Firing was measured in the 500 ms epoch following the last VTA pulse in all sweeps, and compared among experimental groups. At the end of the experiment, animals were killed with anesthesia overdose, and their brains removed for histological verification of lesion status and electrode placement.

Mismatch Negativity

NVHL, NAC-treated NVHL, and sham female rats were implanted with chronic EEG electrodes under isoflurane anesthesia. Electrodes were constructed with 2 mm diameter silver disks coated with silver chloride, and glued on top of bregma, a location equivalent to human vertex, and the contacts led to an *Omnetics* connector on top of the head. Upon a 4-week recovery, rats were first habituated to the recording chamber, a 30 x 50 cm plexiglass box enclosed within a stainless steel box. NNM sessions consisted of exposing the rat to approximately 2,000 tones at two different frequencies (7 or 9 kHz; 30 ms duration) separated by 400 ms, with 95% of the repetitions at one frequency (standard) and 5% at the other frequency (deviant). Tones were delivered with a speaker mounted inside the

enclosure using a TDT RZ6 system (Tucker Davis), and were counterbalanced so half of the time the deviant was either frequency. EEG signals were acquired using a 32 channel Omniplex system (Plexon Instruments) at 1 kHz sampling rate. For analysis, 300 ms epochs around the tone were selected, filtered at 1-30 Hz, baseline-corrected to the 100 ms prior to the stimulus, and averaged separately for standard and deviant tones. A difference wave was constructed by subtracting the standard wave from the deviant wave, and MMN was quantified by measuring the area under the curve in the period between 35 and 100 ms after the stimulus. All rats were exposed to three sessions in three different days, and values were averaged across sessions for every animal.

Prepulse inhibition

Starting at P60, both male and female rats were tested for PPI, as described previously (Feleder et al., 2010). As PPI deficits in NVHL rats are most evident when rats are challenged with apomorphine (Lipska et al., 1995), we injected apomorphine (0.1 mg/kg, i.p.) immediately prior to the PPI test session. Rats were placed in a sound-attenuated startle chamber (San Diego Instruments, San Diego, CA) with a 70 dB background white noise. After a 5 min adaptation period, the PPI test was initiated with pseudorandom trials every 15 to 25 sec. Either pulse (120 dB), prepulse (75 dB, 80 dB, or 85 dB), no pulse or prepulse + pulse were delivered. Trials lasted 23 min and 8 to 10 repetitions of pulse or prepulse + pulse trials were acquired, while null or prepulse only trials were repeated five times for each prepulse amplitude. Startle magnitude was measured using an acceleration-sensitive transducer, and PPI was calculated as the ratio in startle between prepulse + pulse and pulse alone and is expressed as percent reduction. The initial trials (all pulse alone) were used for habituation and not included in the analysis. Trials were excluded from analysis when the animal was moving in the chamber, and sessions were excluded from analysis when startle amplitude was low or more than 50% of trials were excluded for any prepulse + pulse combination. If a PPI session was discarded, rats were tested again a week later.

Statistics—The mean numbers of PV-immunoreactive cells per tissue volume in the ACC were compared among treatment groups using one-way ANOVA followed by post-doc Dunnett multiple comparisons. The mean number of PV-cells, PV-cell intensity, WFA-positive PV and WFA-positive intensity, the overall 8-oxo-dG, and WFA labelling were compared among groups using multivariate ANOVA (Wilk's Lambda) followed by post-hoc Dunnett test for multiple comparisons. Electrophysiology data were compared using a 1-way ANOVA with group as between-subject variable. PPI data were compared using a repeated-measures 2-way ANOVA with lesion status and treatment as between-subject variables, and prepulse intensity as within-subject variable.

Supplementary Material

Refer to Web version on PubMed Central for supplementary material.

Acknowledgments

The authors would like to thank Alex Hernandez, Meredyth Wegener, Christopher Schiefer, Kimberly Konka, Adeline Cottier, and Rudolf Kraftsik for excellent technical assistance. Supported by a NARSAD Distinguished Investigator Award (PO'D), NIH grant R01 MH057683 (PO'D) and Swiss National Science Foundation (#

310030_135736/1 (KQD); National Center of Competence in Research (NCCR) “SYNAPSY - The Synaptic Bases of Mental Diseases” n° 51AU40_125759) and the Avina and Damm-Etienne Foundations (KQD). Patricio O'Donnell is employee and stockholder at Pfizer, inc. Jonathan Kil is employee at Sound Pharmaceuticals, Ltd.

REFERENCES

Behrens MM, Ali SS, Dao DN, Lucero J, Shekhtman G, Quick KL, Dugan LL. Ketamine-induced loss of phenotype of fast-spiking interneurons is mediated by NADPH-oxidase. Science. 2007; 318:1645–1647. [PubMed: 18063801]

Behrens MM, Ali SS, Dugan LL. Interleukin-6 mediates the increase in NADPH-oxidase in the ketamine model of schizophrenia. The Journal of neuroscience : the official journal of the Society for Neuroscience. 2008; 28:13957–13966. [PubMed: 19091984]

Berk M, Copolov D, Dean O, Lu K, Jeavons S, Schapkaitz I, Anderson-Hunt M, Judd F, Katz F, Katz P, et al. N-acetyl cysteine as a glutathione precursor for schizophrenia--a double-blind, randomized, placebo-controlled trial. Biological psychiatry. 2008; 64:361–368. [PubMed: 18436195]

Bitanihirwe BK, Woo TU. Oxidative stress in schizophrenia: an integrated approach. Neuroscience and biobehavioral reviews. 2011; 35:878–893. [PubMed: 20974172]

Cabungcal JH, Nicolas D, Kraftsik R, Cuenod M, Do KQ, Hornung JP. Glutathione deficit during development induces anomalies in the rat anterior cingulate GABAergic neurons: Relevance to schizophrenia. Neurobiology of disease. 2006; 22:624–637. [PubMed: 16481179]

Cabungcal JH, Steullet P, Kraftsik R, Cuenod M, Do KQ. Early-life insults impair parvalbumin interneurons via oxidative stress: reversal by N-acetylcysteine. Biological psychiatry. 2013a; 73:574–582. [PubMed: 23140664]

Cabungcal JH, Steullet P, Morishita H, Kraftsik R, Cuenod M, Hensch TK, Do KQ. Perineuronal nets protect fast-spiking interneurons against oxidative stress. Proceedings of the National Academy of Sciences of the United States of America. 2013b; 110:9130–9135. [PubMed: 23671099]

Carmeli C, Knyazeva MG, Cuenod M, Do KQ. Glutathione precursor N-acetyl-cysteine modulates EEG synchronization in schizophrenia patients: a double-blind, randomized, placebo-controlled trial. PloS one. 2012; 7:e29341. [PubMed: 22383949]

Chambers, RA.; Lipska, BK. A method to the madness: producing the neonatal ventral hippocampal lesion rat model of schizophrenia.. In: O'Donnell, P., editor. Animal Models of Schizophrenia and Related Disorders. Humana Press; New York: 2011. p. 1-24.

das Neves Duarte JM, Kulak A, Gholam-Razaee MM, Cuenod M, Gruetter R, Do KQ. N-acetylcysteine normalizes neurochemical changes in the glutathione-deficient schizophrenia mouse model during development. Biological psychiatry. 2012; 71:1006–1014. [PubMed: 21945305]

Do KQ, Cabungcal JH, Frank A, Steullet P, Cuenod M. Redox dysregulation, neurodevelopment, and schizophrenia. Curr Opin Neurobiol. 2009; 19:220–230. [PubMed: 19481443]

Do KQ, Trabesinger AH, Kirsten-Kruger M, Lauer CJ, Dydak U, Hell D, Holsboer F, Boesiger P, Cuenod M. Schizophrenia: glutathione deficit in cerebrospinal fluid and prefrontal cortex in vivo. The European journal of neuroscience. 2000; 12:3721–3728. [PubMed: 11029642]

Ehrlichman RS, Gandal MJ, Maxwell CR, Lazarewicz MT, Finkel LH, Contreras D, Turetsky BI, Siegel SJ. N-methyl-d-aspartic acid receptor antagonist-induced frequency oscillations in mice recreate pattern of electrophysiological deficits in schizophrenia. Neuroscience. 2009; 158:705–712. [PubMed: 19015010]

Feleder C, Tseng KY, Calhoon GG, O'Donnell P. Neonatal intrahippocampal immune challenge alters dopamine modulation of prefrontal cortical interneurons in adult rats. Biological psychiatry. 2010; 67:386–392. [PubMed: 19914600]

Gawryluk JW, Wang JF, Andreazza AC, Shao L, Young LT. Decreased levels of glutathione, the major brain antioxidant, in post-mortem prefrontal cortex from patients with psychiatric disorders. The international journal of neuropsychopharmacology / official scientific journal of the Collegium Internationale Neuropsychopharmacologicum. 2011; 14:123–130.

Geyer MA, Braff DL. Startle habituation and sensorimotor gating in schizophrenia and related animal models. Schizophrenia bulletin. 1987; 13:643–668. [PubMed: 3438708]

Giovanoli S, Engler H, Engler A, Richetto J, Voget M, Willi R, Winter C, Riva MA, Mortensen PB, Schedlowski M, Meyer U. Stress in puberty unmasks latent neuropathological consequences of prenatal immune activation in mice. Science. 2013; 339:1095–1099. [PubMed: 23449593]

Gysin R, Kraftsik R, Sandell J, Bovet P, Chappuis C, Conus P, Deppen P, Preisig M, Ruiz V, Steullet P, et al. Impaired glutathione synthesis in schizophrenia: convergent genetic and functional evidence. Proceedings of the National Academy of Sciences of the United States of America. 2007; 104:16621–16626. [PubMed: 17921251]

Haddad JJ. Antioxidant and prooxidant mechanisms in the regulation of redox(y)-sensitive transcription factors. Cellular signalling. 2002; 14:879–897. [PubMed: 12220615]

Hartig W, Brauer K, Bigl V, Bruckner G. Chondroitin sulfate proteoglycan-immunoreactivity of lectin-labeled perineuronal nets around parvalbumin-containing neurons. Brain research. 1994; 635:307–311. [PubMed: 8173967]

Hensch TK. Critical period plasticity in local cortical circuits. Nature reviews Neuroscience. 2005; 6:877–888.

Javitt DC, Doneshka P, Zylberman I, Ritter W, Vaughan HG Jr. Impairment of early cortical processing in schizophrenia: an event-related potential confirmation study. Biological psychiatry. 1993; 33:513–519. [PubMed: 8513035]

Johnson AW, Jaaro-Peled H, Shahani N, Sedlak TW, Zoubovsky S, Burruss D, Emiliani F, Sawa A, Gallagher M. Cognitive and motivational deficits together with prefrontal oxidative stress in a mouse model for neuropsychiatric illness. Proceedings of the National Academy of Sciences of the United States of America. 2013; 110:12462–12467. [PubMed: 23840059]

Jones DP, Go YM. Redox compartmentalization and cellular stress. Diabetes Obes Metab. 2010; 12(Suppl 2):116–125. [PubMed: 21029308]

Kasai H. Analysis of a form of oxidative DNA damage, 8-hydroxy-2′-deoxyguanosine, as a marker of cellular oxidative stress during carcinogenesis. Mutat Res. 1997; 387:147–163. [PubMed: 9439711]

Kil J, Pierce C, Tran H, Gu R, Lynch ED. Ebselen treatment reduces noise induced hearing loss via the mimicry and induction of glutathione peroxidase. Hearing research. 2007; 226:44–51. [PubMed: 17030476]

Lavoie S, Murray MM, Deppen P, Knyazeva MG, Berk M, Boulat O, Bovet P, Bush AI, Conus P, Copolov D, et al. Glutathione precursor, N-acetyl-cysteine, improves mismatch negativity in schizophrenia patients. Neuropsychopharmacology : official publication of the American College of Neuropsychopharmacology. 2008; 33:2187–2199. [PubMed: 18004285]

Lee H, Dvorak D, Kao HY, Duffy AM, Scharfman HE, Fenton AA. Early cognitive experience prevents adult deficits in a neurodevelopmental schizophrenia model. Neuron. 2012; 75:714–724. [PubMed: 22920261]

Lewis BL, O'Donnell P. Ventral tegmental area afferents to the prefrontal cortex maintain membrane potential ‘up’ states in pyramidal neurons via D_1 dopamine receptors. Cerebral cortex. 2000; 10:1168–1175. [PubMed: 11073866]

Lewis DA, Curley AA, Glausier JR, Volk DW. Cortical parvalbumin interneurons and cognitive dysfunction in schizophrenia. Trends in neurosciences. 2012; 35:57–67. [PubMed: 22154068]

Lipska BK, Halim ND, Segal PN, Weinberger DR. Effects of reversible inactivation of the neonatal ventral hippocampus on behavior in the adult rat. The Journal of neuroscience : the official journal of the Society for Neuroscience. 2002; 22:2835–2842. [PubMed: 11923448]

Lipska BK, Swerdlow NR, Geyer MA, Jaskiw GE, Braff DL, Weinberger DR. Neonatal excitotoxic hippocampal damage in rats cause post-pubertal changes in prepulse inhibition of startle and its disruption by apomorphine. Psychopharmacol. 1995; 132:303–310.

Moussawi K, Pacchioni A, Moran M, Olive MF, Gass JT, Lavin A, Kalivas PW. NAcetylcysteine reverses cocaine-induced metaplasticity. Nature neuroscience. 2009; 12:182–189.

Muller A, Cadenas E, Graf P, Sies H. A novel biologically active seleno-organic compound--I. Glutathione peroxidase-like activity in vitro and antioxidant capacity of PZ 51 (Ebselen). Biochemical pharmacology. 1984; 33:3235–3239. [PubMed: 6487370]

Niwa M, Kamiya A, Murai R, Kubo K, Gruber AJ, Tomita K, Lu L, Tomisato S, Jaaro-Peled H, Seshadri S, et al. Knockdown of DISC1 by in utero gene transfer disturbs postnatal dopaminergic

maturation in the frontal cortex and leads to adult behavioral deficits. Neuron. 2010; 65:480–489. [PubMed: 20188653]

Nwokocha CR, Baker A, Douglas D, McCalla G, Nwokocha M, Brown PD. Apocynin ameliorates cadmium-induced hypertension through elevation of endothelium nitric oxide synthase. Cardiovascular toxicology. 2013; 13:357–363. [PubMed: 23703608]

O'Donnell P. Adolescent onset of cortical disinhibition in schizophrenia: insights from animal models. Schizophrenia bulletin. 2011; 37:484–492. [PubMed: 21505115]

O'Donnell P. Cortical disinhibition in the neonatal ventral hippocampal lesion model of schizophrenia: New vistas on possible therapeutic approaches. Pharmacology & therapeutics. 2012a; 133:19–25. [PubMed: 21839776]

O'Donnell P. Cortical interneurons, immune factors and oxidative stress as early targets for schizophrenia. The European journal of neuroscience. 2012b; 35:1866–1870. [PubMed: 22708597]

O'Donnell, P. How can animal models be better utilized?. In: Silverstein, SM.; Moghaddam, B.; Wykes, T., editors. Schizophrenia: Evolution and Synthesis. MIT Press; Cambridge, MA: 2013. p. 205-216.

O'Donnell P, Lewis BL, Weinberger DR, Lipska BK. Neonatal hippocampal damage alters electrophysiological properties of prefrontal cortical neurons in adult rats. Cerebral cortex. 2002; 12:975–982. [PubMed: 12183396]

Otte DM, Sommersberg B, Kudin A, Guerrero C, Albayram O, Filiou MD, Frisch P, Yilmaz O, Drews E, Turck CW, et al. N-acetyl cysteine treatment rescues cognitive deficits induced by mitochondrial dysfunction in G72/G30 transgenic mice. Neuropsychopharmacology : official publication of the American College of Neuropsychopharmacology. 2011; 36:2233–2243. [PubMed: 21716263]

Pawlas N, Malecki A. Effects of ebselen on glutathione level in neurons exposed to arachidonic acid and 4-hydroxynonenal during simulated ischemia in vitro. Pharmacological reports : PR. 2007; 59:708–714. [PubMed: 18195460]

Paxinos, G.; Watson, C. The rat brain in stereotaxic coordinates. Fourth Edition edn. Academic Press; San Diego: 1998.

Radi R. Nitric oxide, oxidants, and protein tyrosine nitration. Proceedings of the National Academy of Sciences of the United States of America. 2004; 101:4003–4008. [PubMed: 15020765]

Schmitz C, Hof PR. Design-based stereology in neuroscience. Neuroscience. 2005; 130:813–831. [PubMed: 15652981]

Steullet P, Cabungcal JH, Kulak A, Kraftsik R, Chen Y, Dalton TP, Cuenod M, Do KQ. Redox dysregulation affects the ventral but not dorsal hippocampus: impairment of parvalbumin neurons, gamma oscillations, and related behaviors. The Journal of neuroscience : the official journal of the Society for Neuroscience. 2010; 30:2547–2558. [PubMed: 20164340]

Steullet P, Neijt HC, Cuenod M, Do KQ. Synaptic plasticity impairment and hypofunction of NMDA receptors induced by glutathione deficit: relevance to schizophrenia. Neuroscience. 2006; 137:807–819. [PubMed: 16330153]

Tosic M, Ott J, Barral S, Bovet P, Deppen P, Gheorghita F, Matthey ML, Parnas J, Preisig M, Saraga M, et al. Schizophrenia and oxidative stress: glutamate cysteine ligase modifier as a susceptibility gene. Am J Hum Genet. 2006; 79:586–592. [PubMed: 16909399]

Tseng KY, Chambers RA, Lipska BK. The neonatal ventral hippocampal lesion as a heuristic neurodevelopmental model of schizophrenia. Behavioural brain research. 2009; 204:295–305. [PubMed: 19100784]

Tseng KY, Lewis BL, Hashimoto T, Sesack SR, Kloc M, Lewis DA, O'Donnell P. A neonatal ventral hippocampal lesion causes functional deficits in adult prefrontal cortical interneurons. The Journal of neuroscience : the official journal of the Society for Neuroscience. 2008; 28:12691–12699. [PubMed: 19036962]

Tseng KY, O'Donnell P. D2 dopamine receptors recruit a GABA component for their attenuation of excitatory synaptic transmission in the adult rat prefrontal cortex. Synapse. 2007; 61:843–850. [PubMed: 17603809]

Umbricht D, Schmid L, Koller R, Vollenweider FX, Hell D, Javitt DC. Ketamine-induced deficits in auditory and visual context-dependent processing in healthy volunteers: implications for models of cognitive deficits in schizophrenia. Archives of general psychiatry. 2000; 57:1139–1147. [PubMed: 11115327]

Yao JK, Keshavan MS. Antioxidants, redox signaling, and pathophysiology in schizophrenia: an integrative view. Antioxidants & redox signaling. 2011; 15:2011–2035. [PubMed: 21126177]

Yao JK, Leonard S, Reddy RD. Increased nitric oxide radicals in postmortem brain from patients with schizophrenia. Schizophrenia bulletin. 2004; 30:923–934. [PubMed: 15954198]

Highlights

- Presymptomatic antioxidant treatment prevents loss of parvalbumin in NVHL rats
- Antioxidant treatment prevents altered prefrontal electrophysiology in NVHL rats
- Prepulse inhibition deficits are prevented by antioxidants

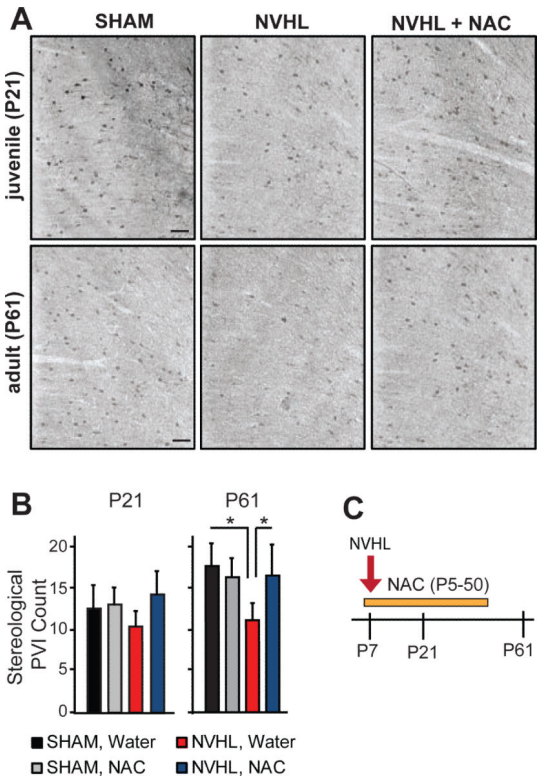

Figure 1. A NVHL blocks the adolescent increase in PV interneuron labeling in the PFC

(A) Representative micrographs of prefrontal PV staining in juvenile (P21) and adult (P61) SHAM, NVHL, and NAC-treated NVHL rats. Scale bar is 80 μm. See Suppl. Fig 1 for lesion extent. (B) Bar graphs illustrating PV cell counts using unbiased stereology at P21 (left) and P61 (right) in all four treatment groups. PV cell count increased between P21 and P61 in SHAM, but not in NVHL rats. Juvenile NAC treatment rescued the progression in PV cell numbers in NVHL rats. ANOVA $F_{(5,36)}$=4.7, p=0.002. Age: $F_{(1,36)}$=10.2, p=0.003, Lesion: $F_{(1,36)}$=1.36, p=0.11, Lesion x Age: $F_{(1,36)}$=6.7, p=0.014, Treatment: $F_{(1,36)}$=3.9, p=0.057, Treatment x Age: n.s. (C) Diagram illustrating the time course of NAC treatment and juvenile (P21) and adult (P61) assessments. In this and all other figures, data are expressed as mean ± SEM, *p<0.05.

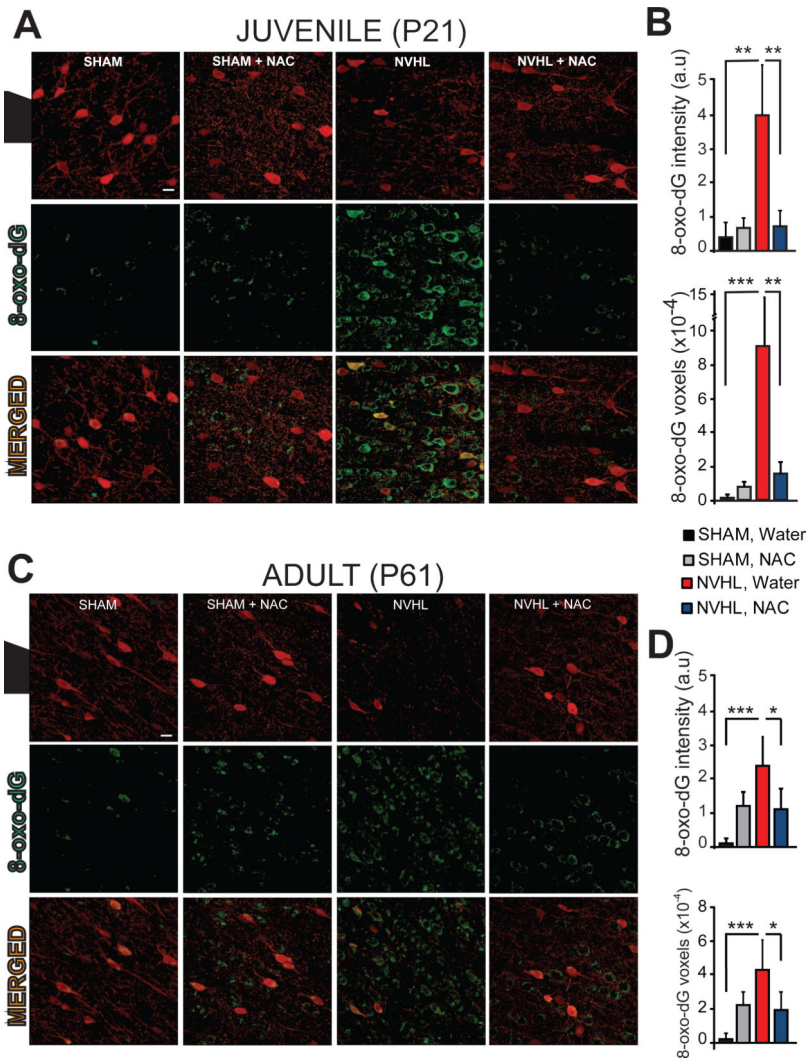

Figure 2. Oxidative stress shown with 8-oxo-dG in the PFC of NVHL rats

(A) Representative micrographs showing double labeling for PV (red) and 8-oxo-dG (green) in the PFC in the four groups at P21. Scale bar is 10 μm. (B) Summary of the datashowing that an NVHL causes a massive increase in 8-oxo-dG labeling in the PFC at P21 that is prevented with juvenile NAC treatment. Top graph illustrates 8-oxo-dG fluorescence intensity and the bottom graph quantifies the number of labeled voxels in each group. ANOVA for 8-oxo-dG intensity: $F_{(3,14)}$=13.7, p=0.00002, Lesion $F_{(1,14)}$=18.4, p=0.008, Treatment $F_{(1,14)}$=9.6, p=0.008, Lesion x Treatment $F_{(1,14)}$=13.0, p=0.003. (C) Representative micrographs showing double labeling for PV (red) and 8-oxo-dG (green) in the PFC at P61. Scale bar is 10 μm. (D) Summary of the data showing that the NVHL increases 8-oxo-dG in the PFC at P61, which is prevented with juvenile NAC treatment. ANOVA for 8-oxo-dG intensity: $F_{(3,18)}$=7.8, p=0.001, Lesion $F_{(1,18)}$=12.5, p=0.002, Treatment $F_{(1,18)}$=0.13, p=n.s., Lesion x Treatment $F_{(1,18)}$=10.8, p=0.004.

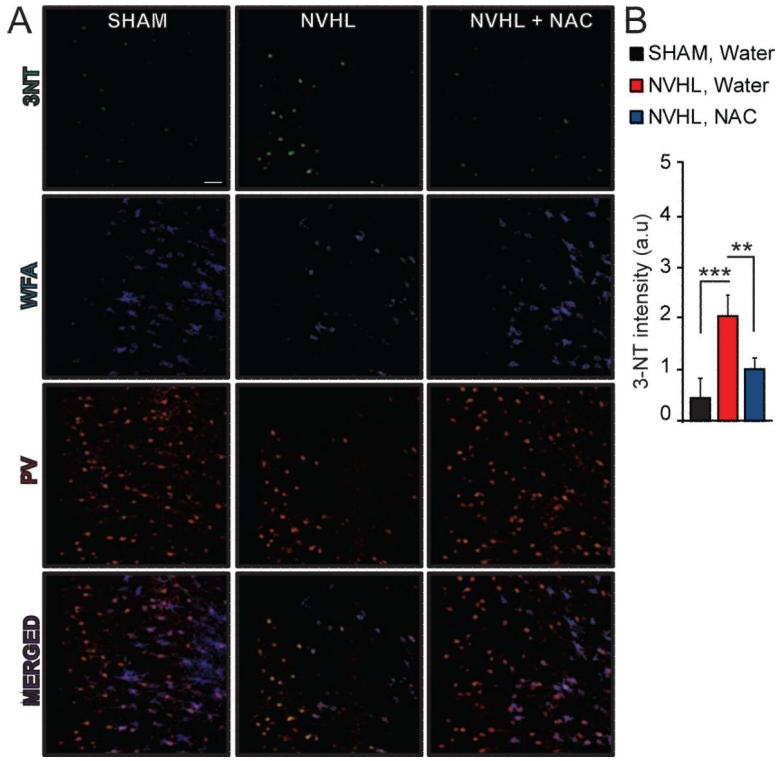

Figure 3. Oxidative stress in the PFC of adult NVHL rats shown with 3-NT

(A) Representative micrographs showing triple labeling for 3-NT (green), WFA (blue) and PV (red) in the three groups. Scale bar is 100 μm. b, (B) Summary of the data showing that an NVHL causes a significant increase in 3-NT labeling in the PFC at P61 that is prevented with juvenile NAC treatment. Top graph illustrates 3-NT fluorescence intensity in each group. One-way ANOVA for 3-NT intensity revealed a very significant effect of treatment ($F_{(2,53)}$=85.2, p<0.0001). Comparisons between each pairs using Tukey-Kramer also showed significant differences (P<0.0001) for SHAM versus NVHL and NVHL versus NAC.

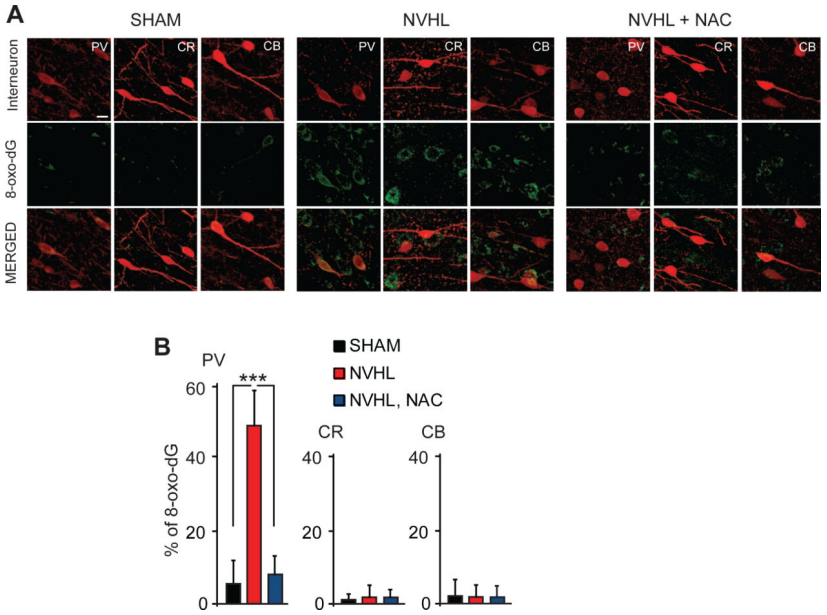

Figure 4. The NVHL causes increased oxidative stress in PV, but not CR and CB interneurons, which is prevented by developmental NAC treatment

(A) Micrographs showing 8-oxo-dG labeling (green) of parvalbumin (PV)-, calretinin (CR)- and calbindin (CB)-positive interneurons (red) in the PFC of SHAM, NVHL and NAC-treated NVHL rats. Scale bar is 10 μm. (B) Summary of the data. In PV interneurons, 8-oxo-dG labeling increased following an NVHL lesion, which was prevented with NAC treatment (Treatment: $F_{(2,65)}=212.97$, $p<0.0001$). ***$p<0.001$.

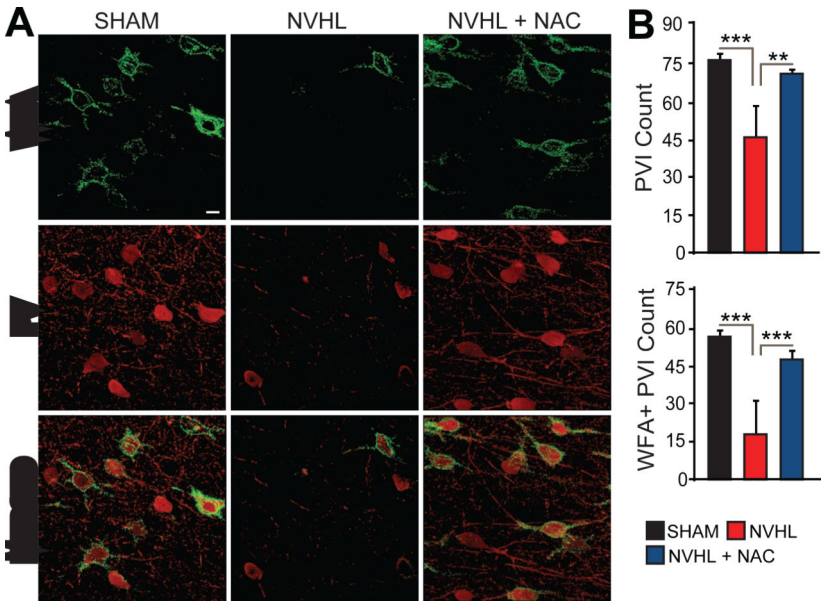

Figure 5. Perineuronal nets (PNN) are reduced in the PFC of adult NVHL rats, but rescued by juvenile NAC treatment

(A) Representative micrographs showing double labeling of PV (red) and *Wisteria floribunda agglutinin* (WFA; green), which labels PNN. Scale bar is 10 μm. (B) Plots illustrating PV interneuron (PVI) counts (top) and the number of cells co-labeled with PV and WFA (bottom). PVI count is reduced following an NVHL lesion, and this reduction is prevented with juvenile NAC treatment. (Overall effect: $F_{(8,16)}$=3.8, p=0.01, PVI count: $F_{(2,11)}$=15.3, p<0.0007). The number of WFA PVI decreases in NVHL rats compared to controls, and this reduction is prevented with juvenile NAC treatment (PNN count: $F_{(2,11)}$=28.5, p<0.0001). **p<0.01, ***p<0.001.

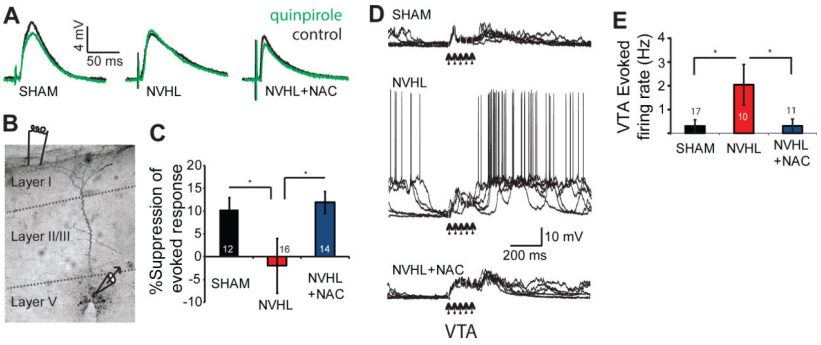

Figure 6. Electrophysiological deficits are rescued by NAC treatment in NVHL rats

(A) Representative traces of excitatory post-synaptic potentials (EPSP) evoked by superficial layer electrical stimulation in adult PFC before (black trace) and after (green trace) bath application of the D2-agonist quinpirole (5 μM). (B) Neurobiotin-filled layer V pyramidal cell in the PFC; the relative position of the bipolar stimulating electrode and the recording electrode are shown schematically. (C) Bar graphs illustrating the magnitude of EPSP attenuation by quinpirole in slices from SHAM, NVHL, and NAC-treated NVHL rats. In sham rats, quinpirole reduces the size of the synaptic response, whereas in NVHL rats this attenuation is absent. NAC treatment during development reverses this deficit in NVHL animals (ANOVA: $F_{(2,39)}$=3.328, p=0.046). (D) Traces from *in vivo* intracellular recordings in PFC pyramidal neurons showing responses to electrical stimulation of the ventral tegmental area (VTA) with trains of 5 pulses at 20 Hz in anesthetized SHAM (top), NVHL (middle), and NAC-treated NVHL (bottom) rats. Each panel is an overlay of 5 traces that illustrate the representative type of response observed in each group, with NVHL showing enhanced firing following VTA stimulation, while firing is sparse in SHAM and NAC-treated NVHL rats. (E) Bar graph illustrating group data for action potential firing in the 500 ms epoch following VTA stimulation in all three groups. ANOVA: $F_{(2,37)}$=4.5, p<0.05; NVHL firing was higher than in shams (post-hoc Tukey's q=3.9, p<0.05) and higher than in NAC-treated NVHL rats (post-hoc Tukey's q=3.6, p<0.05). In all electrophysiology experiments data from SHAM and NAC-treated SHAM rats were combined as they did not show differences.

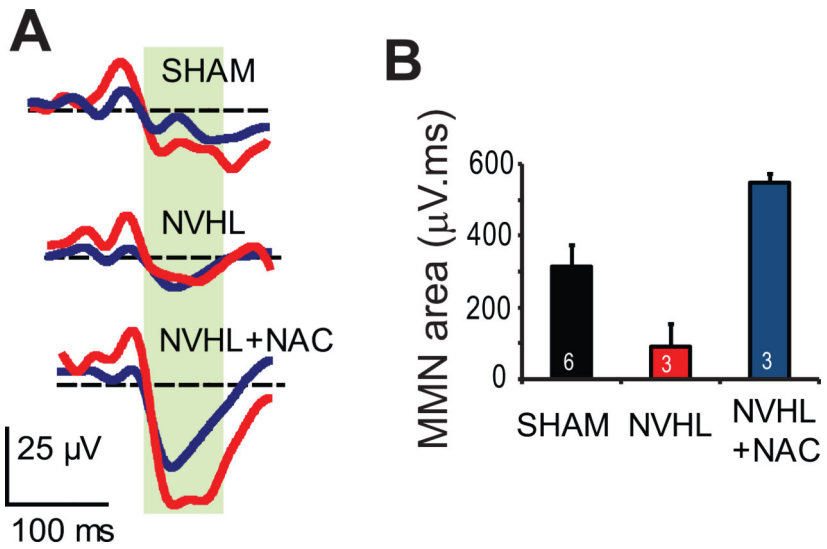

Figure 7. Mismatch negativity (MMN) deficits are rescued by NAC treatment

(A) Representative traces of auditory evoked potentials from standard (blue) and deviant (red) stimuli in a sham (n=6; top), NVHL (n=3; middle), and NAC-treated NVHL rat (n=3; bottom). The green box highlights the epoch in which the negativity was measured (35-100 ms following the stimulus). All traces are averages of at least 80 repetitions. (B) Group data comparing MMN measured as the area under the curve in the highlighted region reveal a significant difference among groups (ANOVA: $F_{(2,11)}$=9.742; p=0.006). The data illustrated are averages from 3 different sessions in each rat. A post-hoc comparison between NVHL and NVHL+NAC revealed a significant difference (Bonferroni test; p=0.005).

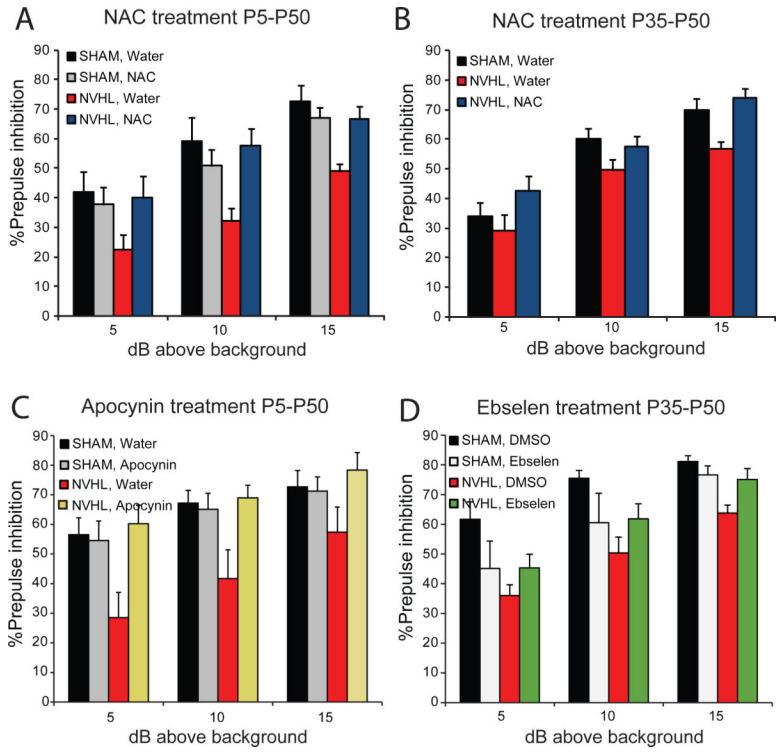

Figure 8. Prepulse inhibition deficits were rescued with antioxidant treatment

(A) Prepulse inhibition deficits were observed in NVHL rats when challenged with apomorphine (0.1 mg/kg, i.p.). This deficit was completely reversed with juvenile NAC treatment (Lesion: $F_{(1,42)}$=3.529 p=0.067, Treatment: $F_{(1,42)}$=1.644, p=0.207, Lesion x Treatment: $F_{(1,42)}$=5.730, p=0.021). n=12-16, * p<0.05 compared to NVHL. (B) In another group of rats, NAC was administered starting at P35, stopped at P50, and the rats tested for PPI at P61. The bar graph illustrates PPI at three different prepulse intensities in this group with adolescent NAC treatment. ANOVA: group effect $F_{(2,28)}$=3.364, p<0.045; post-hoc tests revealed only a trend for a difference in PPI in NVHL compared to SHAM (LSD, p=0.069), and a significant difference between NVHL and NAC-treated NVHL (LSD, p=0.016). (C) Some animals received ebselen from P35 and were tested for PPI at P61. There was a significant lesion effect ($F_{(1,28)}$=7.11; p=0.013) and a significant lesion status by treatment interaction ($F_{(1,28)}$=7.09; p=0.013). (D) Another set of animals received apocynin and were tested for PPI. We observed a significant lesion by treatment interaction ($F_{(1,25)}$=4.8; p=0.038).